KRONOS FUSION ENERGY

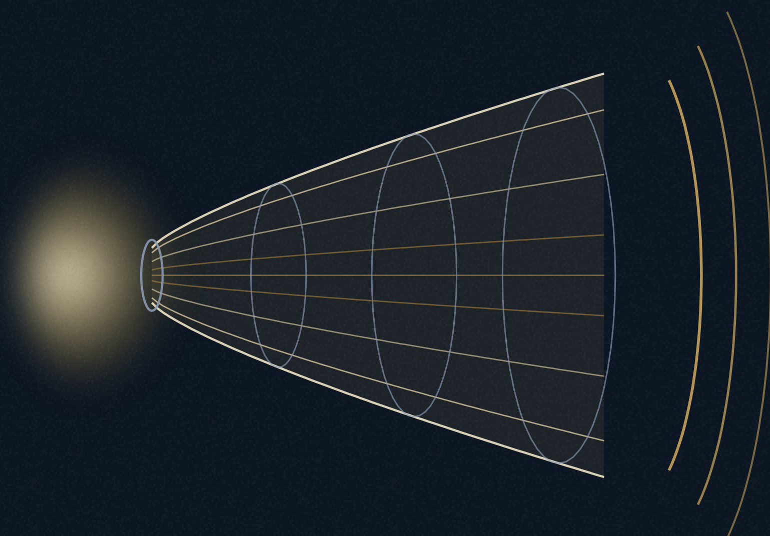

PAPER IV OF THE 2026 KRONOS SET

Direct Energy Conversion

A Quasineutral Expander

For a D–^{3}He magnetic-mirror burner: the electron channel is the larger axial stream, and a quasineutral expander can recover it.

D–^{3}He mirror · axial split 55.5 / 44.5% · cascade η 0.563 · expander ×20

Explore it live — 3-D model · physics validator · film series

PREPARED BY P. I. FORD · G. L. KULCINSKI

2026 · EDITORIAL

KRONOS FUSION ENERGY · 2026

The Kronos Fleet

Fuel follows purpose, not platform.

Hyperion · Aegis · MetroVolt

THE OFFICIAL RECORD

What this document is, and how to read its numbers

This is a combined editorial. It gathers, in one volume, the two design studies Kronos Fusion Energy released in 2026 — a compact spherical-tokamak tritium/helium-3 breeder and a deuterium–helium-3 tandem-mirror generator — together with the intellectual-property estate, the people, and, in the internal edition, the full commercial case. The scientific text is the same text that appears in the arXiv preprints and the journal submissions; the editorial adds the apparatus a reader needs to hold the whole program at once, and nothing in the physics is altered to fit it.

THE HONESTY STANCE IS THE ASSET

Every headline quantity carries an **evidence class** — DERIVED RECOMPUTED MEASURED REQUIREMENT — and, where a number is a modelled extrapolation rather than a demonstrated value, it is labelled as such and its downside is shown next to it. Several quantities in the underlying corpus moved after first publication; where a value has been withdrawn or restated, the record says so plainly. This is deliberate: a diligence team will find the load-bearing assumptions, so the document surfaces them first.

TITLE	The Kronos Fleet — Hyperion · Aegis · MetroVolt: A Combined Design & Commercialization Study
AUTHOR	Priyanca Ford, Founder & CEO, on behalf of Kronos Fusion Energy
EDITION	2026 Combined Editorial · first issue
COMPANION WORKS	The five-paper arXiv drop — (1) Breeder, (2) Burner, (3) REBCO magnet & tape, (4) Direct Energy Conversion, (5) AI/ML/Quantum control — with matching numbered Zenodo deposits, plus the IOP journal and IAEA-FEC submissions. Patents were filed before the drop.
NAMING	Hyperion = the breeder; Aegis (defense) and MetroVolt (data-center) = one generator in two housings. Internal mode letters (D1, L) do not appear on public surfaces.
STATUS	Conceptual design & simulation study. Nothing herein is a construction commitment.

HOW TO READ THIS VOLUME

The fleet at a glance, and the way its numbers are marked

This volume opens with *Orientation*, presents the five research papers as a bound sequence, and closes with the *Apparatus*. *Foundations* sets out the three general results both machines rest on. *Paper One* is the Hyperion breeder; *Paper Two* the Aegis / MetroVolt generator; *Papers Three, Four and Five* are the enabling science — high-field REBCO magnets and tape, direct energy conversion, and the AI / ML / quantum control stack. A *Digital Twin & 3-D Model* part follows, then the *Environmental* profile. The *Economics* and levelized cost and the *Business Case* and diligence record appear in the internal edition only; the *Simulations* proof record and the Apparatus — patent portfolio, team, limitations, and sources — close both editions.

THE FLEET AT A GLANCE

	HYPERION	AEGIS	METROVOLT
Role	Strategic-isotope foundry	Defense installation power	Campus power
Machine	**Spherical tokamak**	**Tandem mirror**	**Tandem mirror**
Fuel	Deuterium–tritium	Deuterium–helium-3	Deuterium–helium-3
Delivers	Tritium · ^{3}He · 14 MeV n	Resilient installation power	Firm campus power
Physics bar	**Fusion gain only**	Closure (gates named)	Closure + lunar ^{3}He
In the fleet	Breeds the fuel	Proves the generator	Commercial destination

HOW THE NUMBERS ARE MARKED

Every headline quantity carries an evidence class — DERIVED from first principles, RECOMPUTED from raw data, MEASURED in hardware, or a REQUIREMENT yet to be met. Financial figures carry a case label and are confined to the internal (confidential) edition. Values that moved after first publication are shown as withdrawn or restated rather than quietly changed. A capability you can evaluate is one whose limits are on the page.

ABSTRACT

Direct Energy Conversion — A Quasineutral Expander

For a deuterium–helium-3 magnetic-mirror burner, the directed axial power splits 55.5% into the electron channel and 44.5% into the ion channel — so the electron stream, not the ion stream, is the larger prize, holding across 20–200 keV. Ion direct conversion of the 14.66 MeV proton is genuine direct energy conversion at measured tube efficiency; the electron/thermal channel is recovered instead with a bottoming cycle. A quasineutral two-species expander — field ratio ~20, ambipolar barrier ~240 keV — lifts axial electric recovery by ~13%. The upside is bounded and honest: Kronos has built no converter.

Companion deposit (code & data, reproducible under CC BY 4.0): DOI 10.5281/zenodo.21842864 · Zenodo community *kronos_fusion_energy*.

Explore it live: interactive 3-D model · run the physics validator · companion film series (the deposited solvers, in the browser).

Keywords: direct energy conversion · magnetic mirror · quasineutral expander · deuterium–helium-3 · charged-power budget

CONTENTS

Table of Contents

NOMENCLATURE

Symbols, units, and the names of things

Q	plasma (fusion) gain, P_{fus}/P_{aux}
Q_E	engineering gain, net electric out / recirculating in
H_{98}	confinement enhancement over the IPB98(y,2) scaling
Z_{eff}	effective ion charge
c_{ee}	electron–electron bremsstrahlung leading coefficient, 2.120022 (exact)
τ_E	energy confinement time
I_p	plasma current
R_0, a	major radius, minor radius
κ, δ	elongation, triangularity
β_N	normalized plasma beta (Troyon-normalized)
TBR	tritium breeding ratio
DEC	direct energy conversion
CF	plant capacity factor (availability)
FOAK / NOAK / BOAK	first / n^{th} / best of a kind
Hyperion	the ST breeder (internal: Mode D2)
Aegis	the generator, defense/installation housing (internal: Mode M)
MetroVolt	the generator, data-center housing (Mode M)

§ 1

The accounting assumption the whole converter train inherits

Direct energy conversion has been part of the advanced-fuel fusion program since the tandem-mirror era, and the argument for it is clean. Deuterium–helium-3 releases **18.35 MeV** into two charged lines — a **14.66 MeV proton** and a **3.67 MeV alpha** — with no neutron in the primary branch. The charged-particle power that streams out of a magnetic mirror's open ends can, in principle, be caught on a biased electrode and turned back into electricity at high efficiency, rather than dumped into a boiler as heat. The venetian-blind collector, the travelling-wave direct converter, and the cusp and ICC ion converters were all built against that promise, and they reach demonstrated net efficiencies in the high forties of a percent. This paper claims none of that train as novel. The ion direct converter is prior art, it works, and it is not what is in question here.

What is in question is a single accounting assumption the entire train inherits. The 14.66 MeV proton carries roughly **80%** of the charged birth energy, and it is tempting to conclude that a good ion converter therefore recovers about 80% of the exhaust at high efficiency, leaving only a small thermal remainder to mop up. That conclusion silently identifies the *birth* spectrum with the *axial loss* spectrum. They are not the same object, and treating them as the same is a category error with a large price attached.

A 14.66 MeV proton born into an 80 keV plasma does not stream out of the machine ballistically, carrying its birth energy to the converter intact. It slows down. Where its birth energy sits relative to the plasma's critical energy decides whether it heats the background ions or the background electrons on the way to the exit — and that decision, followed honestly all the way to the axial loss cone, is the whole of this paper's first result. It inverts the picture the converter train was built on: at reactor temperature the dominant axial stream is not a beam of fast protons a grid stack can decelerate, but a directed *electron* stream that no published converter is designed to catch.

> **THE THREE CLAIMS OF THIS PAPER, STATED PLAINLY**
>
> **One:** at a reactor ion temperature of 80 keV the thermalized axial exit carries a **55.5% electron / 44.5% ion** split — the electron/thermal channel is the *larger* stream, holding across 20–200 keV. **Two:** no established converter recovers a directed electron stream; the hot-emitter route is walled off by its own thermionics. **Three:** a quasineutral two-species *expander* — the ambipolar magnetic nozzle run backward — recovers a bounded **≈28%** of that electron channel without ever raising a space-charge wall. And the honest coda: this lifts axial electric recovery by **≈13%** (**≈97 MW$_e$**) but moves plant Q_E only from 1.0023 to 1.0026. DEC is a bounded upside lever, not the burner's closure mechanism.

Every quantitative claim below is tagged by its evidence basis, on the same terms the source paper uses: **measured** or **derived** (from established slowing-down theory, Richardson–Dushman thermionics, or the measured converter record), **theory / design-study**, and **open-risk** where a number rests on a loss term that has not yet been measured for this application. One boundary condition frames the entire document: **Kronos has built no converter.** The expander is a proposed topology with a pre-registered bench experiment attached, not a device on a test stand. The operating point at 80 keV is carried throughout as a *labeled extrapolation* — it is the burner's own design point, stated as such, not a demonstrated plasma.

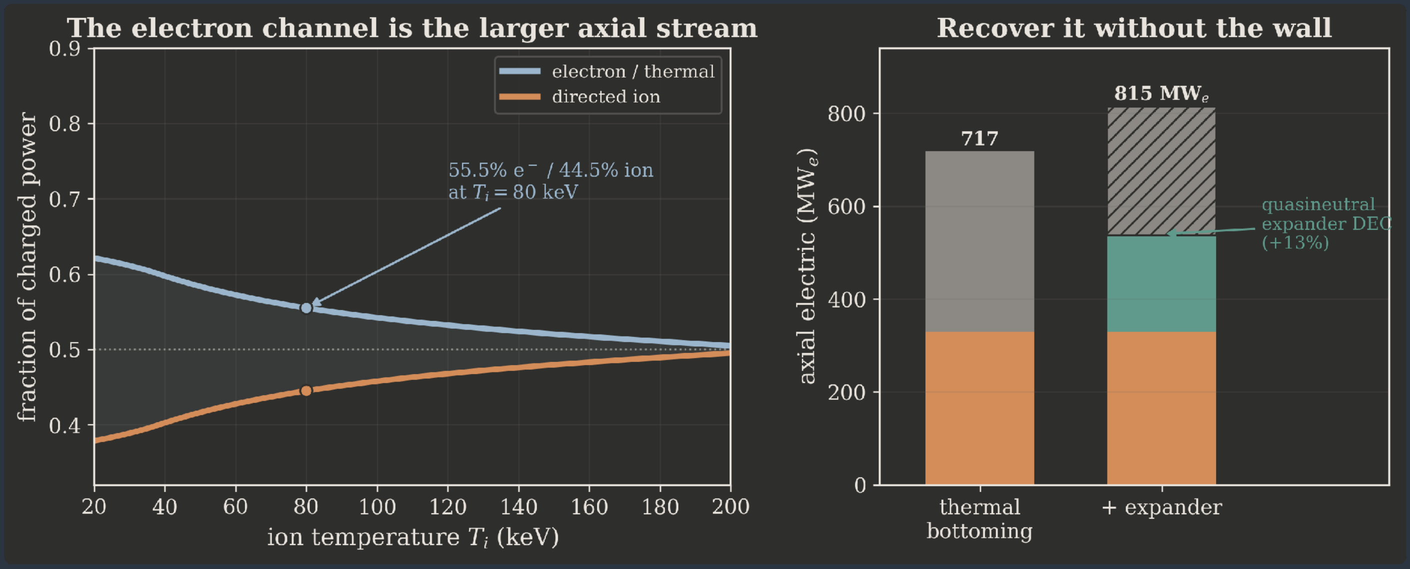

FIGURE 1. The argument on one spread. At a reactor ion temperature of 80 keV the 14.66 MeV D–³He proton thermalizes onto the electrons, so the axial exit carries a 55.5% electron / 44.5% ion split — the electron/thermal channel is the *larger* stream, inverting the received picture (left). No converter recovers a directed electron stream; a quasineutral two-species expander — the ambipolar magnetic nozzle run backward — recovers ≈28% of it without the back-emission wall, lifting axial electric recovery ≈13% (right). Q_E barely moves: DEC is a bounded upside, not the burner's closure. DERIVED

§ 2

The thermalized axial split — the electron channel is the larger stream

The energy partition of a fast ion slowing in a plasma is fixed by the **Stix critical energy** E_c. Above E_c the ion drags predominantly on the electrons; below it, on the background ions. This is textbook slowing-down theory, and it is not in dispute. For a 50:50 D:^{3}He mixture at T_e = 80 keV, the proton's critical energy is **≈0.85 MeV**. The 14.66 MeV proton is therefore born **≈17× above its critical energy**, and it delivers the large majority of its energy to the electrons on the way down. A pure, full-slowing-down accounting — letting every proton thermalize completely before it counts — sends **≈76%** of the charged power to the electron channel.

A mirror, however, does not fully thermalize its fast ions. They escape axially on a confinement time τ_{ax} that competes with the slowing-down time τ_s. An ion that leaks out of the loss cone before it has finished slowing carries its residual directed kinetic energy with it, and that residual stays in the ion channel. The honest axial split is therefore neither the birth spectrum (80% ion) nor the full-slowing-down limit (76% electron) — it lives between them, set by how the escape clock races the slowing clock.

We book that race with a single control ratio,

CONTROL RATIO	$\kappa = \tau_{ax} / \tau_s$ — axial confinement time over slowing-down time
CALIBRATION	κ ≈ **0.50** reproduces the burner's canonical operating-point split at 80 keV
REGIME	κ < 1 — a physically sensible mirror in which ions escape *before* fully slowing

Integrating the coupled slowing-down and escape problem, with residual directed energy kept in the ion channel, and calibrating κ to reproduce the simulator's canonical split gives **κ ≈ 0.50** — a physically sensible mirror regime, not a fitted extreme. The result is the inversion:

55.5%
ELECTRON / THERMAL CHANNEL
the larger axial stream at 80 keV

44.5%
DIRECTED-ION CHANNEL
residual directed energy at escape

≈17×
PROTON BIRTH VS. E_C
14.66 MeV over ≈0.85 MeV

At the 80 keV operating point the electron/thermal channel carries **55.5%** of the axial charged power and the directed-ion channel **44.5%** — and the electron channel remains the larger stream across the entire **20–200 keV** range (Figure 2). This is not a subtle rebalancing; it is a reversal of which stream a converter designer should be aiming at. The whole ion-DEC train was built to catch the channel that turns out to be the *smaller* one. DERIVED

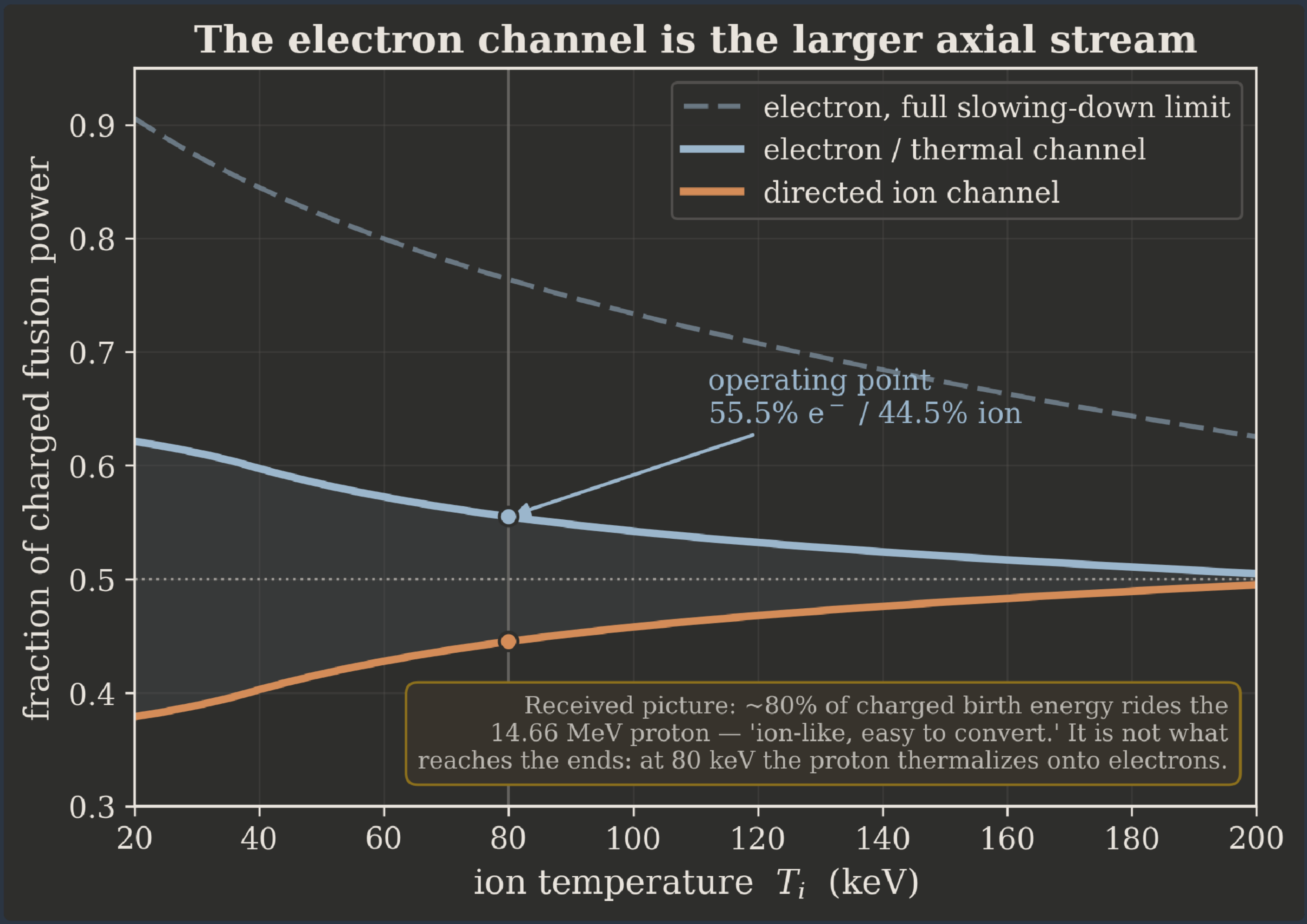

FIGURE 2. Fraction of charged fusion power in each axial channel versus ion temperature. At the 80 keV operating point the electron/thermal channel carries 55.5% and the directed-ion channel 44.5%; the electron channel is the larger stream throughout 20–200 keV. The dashed curve is the full-slowing-down limit (≈76% electron). Basis: slowing-down theory (Stix / Gaffey), with κ calibrated to the Kronos simulator operating point. DERIVED

The inversion is not an artifact of any one transport model. It follows from textbook slowing-down theory, and it survives when the confinement ratio κ is swept across the physically reasonable range: the electron channel stays the larger stream in every regime (Figure 3). The calibrated operating point fixes the exact numbers 55.5 / 44.5, but the *direction* of the result — electron-dominant axial loss — does not depend on that calibration at all.

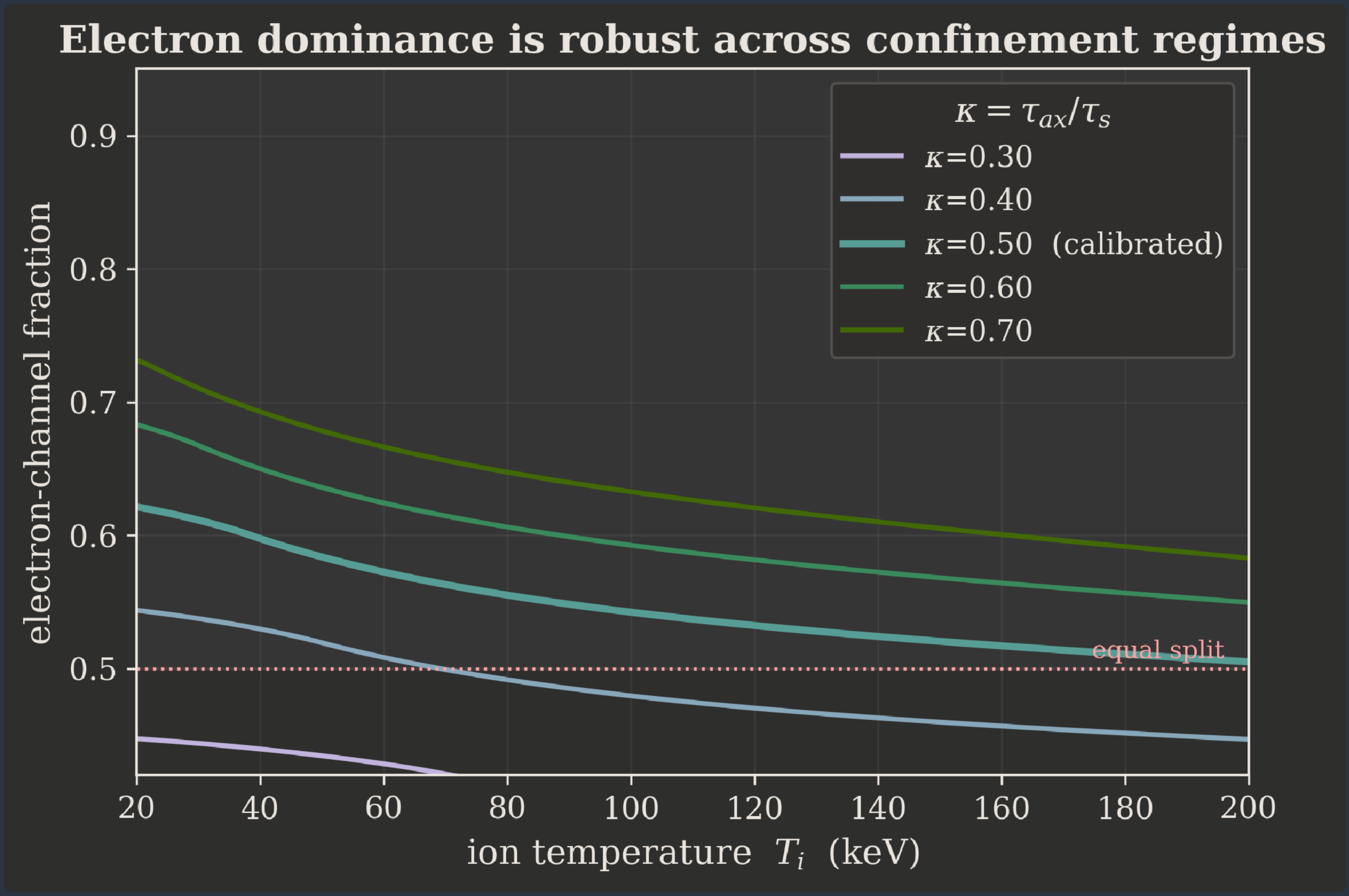

FIGURE 3. Robustness of the electron-dominance result. The electron-channel fraction versus ion temperature for a range of the confinement ratio $\kappa = \tau_{ax}/\tau_s$; the electron channel remains the larger stream across every regime, so the inversion is not an artifact of the calibrated operating point. Basis: slowing-down theory (Stix / Gaffey). DERIVED

The whole ion-DEC train was built to catch the channel that turns out to be the smaller one.

§ 3

The electron-channel gap — and the back-emission wall

Relocating the dominant stream onto the electrons exposes a problem the ion-DEC literature never had to solve: **there is no established converter for a directed electron stream.** This is where the category error becomes expensive. The tempting move — credit the 55.5% electron channel at the same high efficiency the ion converter earns on the ion channel — is not available, because the natural device for the job does not work. The electron/thermal channel must *not* be booked at converter efficiency; doing so would smuggle back exactly the assumption §2 just dismantled.

The obvious candidate is a hot electron collector: a heated surface biased to catch incoming electrons and return their energy to the circuit. It is defeated by its own thermionics. A surface hot enough to matter emits a Richardson–Dushman back-emission current,

$$J_{back} = 120.17\ T^2\ \exp(-\phi/kT) \quad \text{A cm}^{-2}$$

that, once it exceeds the signal current density it is meant to collect, floods the gap with its own emission and stalls collection entirely. At the burner operating point the signal it must beat is $\boldsymbol{J_{signal}} = \mathbf{0.0125\ A\ cm^{-2}}$ — a small number, and that is the problem. Mapping the ratio J_{back}/J_{signal} over emitter temperature and work function draws a boundary surface (Figure 4): the $R = 1$ contour is the **back-emission wall**, the locus where a hot collector's own emission equals the signal it is trying to read.

> **WHERE EVERY REAL EMITTER LANDS**
>
> The operating band any real low-work-function emitter can reach — LaB_6 / CeB_6, work function **φ ≈ 2.4–2.7 eV**, temperature ***T*** **≈ 1500–1900 K** — sits $\mathbf{10^1}$**–**$\mathbf{10^4}$**× deep** inside the flooded region. The wall is not an engineering detail to be optimized away with a better emitter. It is where a hot directed-electron collector *stops working*, and it is why the electron channel is a genuine open problem rather than a solved one waiting on a vendor.

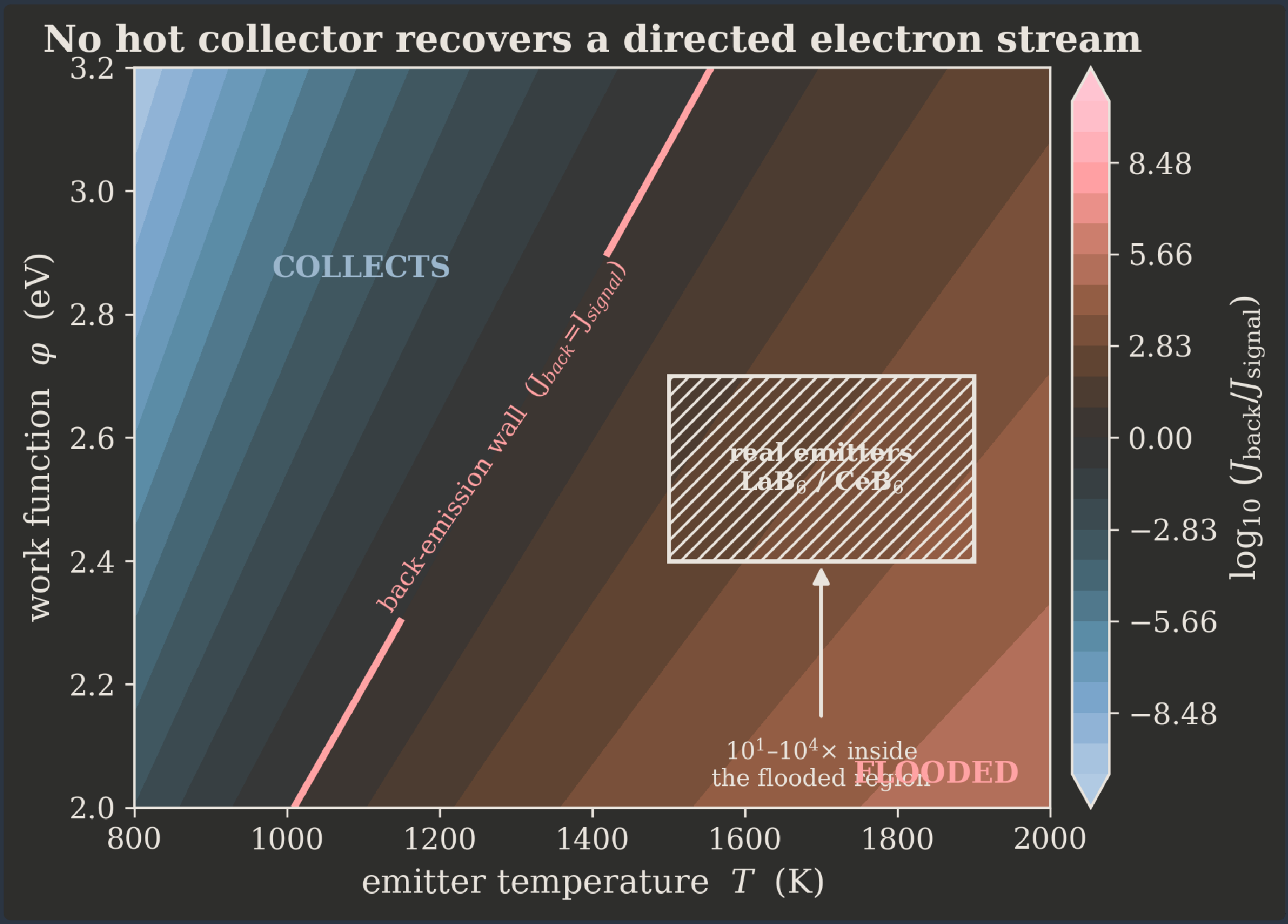

FIGURE 4. The back-emission wall. Contours of $\log_{10}(J_{back}/J_{signal})$ over emitter temperature and work function; the red $R = 1$ contour separates the collecting region from the flooded one. Every real low-work-function emitter (hatched box) lies far inside the flooded region. Basis: Richardson–Dushman DERIVED; J_{signal} is a simulator operating point OPEN-RISK

One honest caveat travels with this figure. J_{signal} is a simulator operating point, not a measured collector value, so it is carried as open-risk. The *conclusion*, however, is robust to it: the real-emitter band floods by one to four orders of magnitude, so even a signal current an order of magnitude larger than assumed would leave every buildable emitter deep inside the wall. The gap does not close by tuning J_{signal}. It closes only by abandoning the hot-emitter topology altogether — which is what §5 does.

§ 4

Prior art, and the corner of the map that is empty

Before proposing a new converter it is worth establishing, carefully, that the record does not already contain one. A citation-grounded sweep of **98 verified primary works** across four subfields — ion direct converters; thermionic and low-work-function emitters; advanced-fuel spectra and thermalization; and adiabatic DEC theory — is reported in the companion literature map. Two negatives survive that sweep, and together they define this paper's contribution (Figure 5).

First negative: no published DEC accounting reports the *thermalized* axial split rather than the birth spectrum. The advanced-fuel reactor-physics literature does build its power balance on the electron energy content — it knows the electrons carry the load — but it stops at the volumetric balance and never propagates that fact to an axial converter split. The converter designers, in turn, inherit the birth spectrum. The two communities each hold half of the correction and neither assembles it.

Second negative: no converter recovers a directed electron stream. The ion converters (venetian-blind, multi-grid, travelling-wave, cusp) recover ions and treat electrons as a suppressible loss to be swept aside. The thermionic community's wall — §3 — is unsolved for a directed stream. And the ambipolar magnetic nozzle, which *does* naturally handle a quasineutral two-species flow, is run **forward**, as a thruster, in every device in the propulsion record. The object that could catch the electron channel exists; it has simply never been pointed the other way.

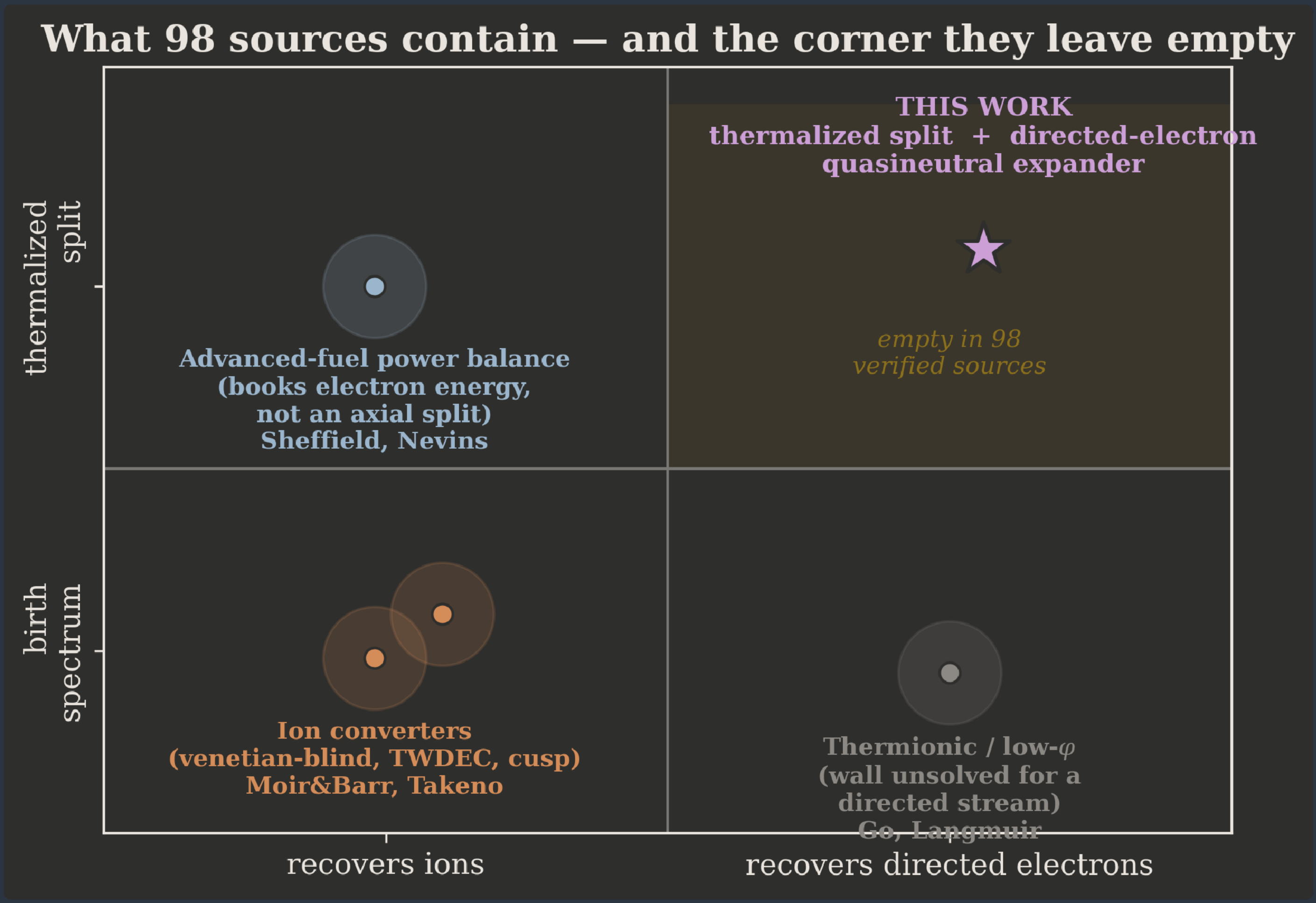

FIGURE 5. The two-gap prior-art map. Published direct-conversion work clusters where this paper disclaims novelty (ion converters; thermionic emitters) and against the birth-spectrum accounting; the corner combining the *thermalized* split with a *directed-electron* converter is empty across 98 verified sources, and is where this work sits. Basis: the companion prior-art ledger. DERIVED

The concept of §5 is the reversal of that last object — the ambipolar nozzle run backward for energy recovery — and it is unanticipated in the surveyed record. Every enabling piece exists individually and is well established: adiabatic energy conversion, the ambipolar potential of a magnetic nozzle, quasineutral two-species flow. None has been assembled in reverse for energy recovery. That empty corner of the map is both the physics contribution and the intellectual-property position. DERIVED

§ 5

A quasineutral two-species expander DEC

The magnetic nozzle already contains the physics we need — it simply runs the wrong way. In a plasma thruster, electron thermal energy is converted through the ambipolar potential into directed ion kinetic energy and exhausted for thrust. We propose to run the same expansion as an *energy-recovery* stage instead of a propulsion stage. The mechanism has three moving parts, all of them established:

ADIABATIC CONVERSION	As the field expands by a ratio $R_{exp} = B_{throat}/B_{exit}$, the invariant $\mu = mv_\perp^2/2B$ converts perpendicular energy into parallel energy — the adiabatic-DEC backbone of Rax, Kolmes & Fisch (2025)
AMBIPOLAR BARRIER	Quasineutrality maintains a potential $e\,\Delta\varphi \approx T_e \ln R_{exp}$ across the expansion
TWO-SPECIES COLLECTION	A biased collector at the exit recovers the directed energy of *both* species; electrons arriving above the barrier are caught at an electrode near the plasma potential

The crucial point is the last one. The electron channel is recovered *against the ambipolar hill*, at an electrode sitting near the plasma potential — so **no hot emitter is ever introduced, and the space-charge wall of §3 never has a chance to form.** The topology sidesteps the wall by construction rather than fighting it. That is what makes it a candidate for the larger axial channel where the hot collector fails.

One fully worked embodiment fixes the numbers:

20	≈240 keV	39%	≈28%
EXPANSION RATIO R_{EXP}	AMBIPOLAR BARRIER $\Delta\Phi$	IDEAL RECOVERY	REALISTIC RECOVERY
B_{throat} 5 T → B_{exit} 0.25 T	at T_e 80 keV, throat	adiabatic limit, no losses	after demagnetization & detachment

At $R_{exp} = 20$ (5 T → 0.25 T) with $T_e = 80$ keV at the throat, the ambipolar barrier is **≈240 keV**. The recoverable electron-channel fraction is **≈39%** in the ideal adiabatic limit and **≈28%** after realistic losses — two loss terms located by the propulsion literature and carried here honestly as open-risk: *finite-gyroradius electron demagnetization* downstream, and *incomplete plasma detachment* from the field. Across $R_{exp} = 2$–60 the realistic recoverable fraction runs **16–70%** (Figure 6).

One further open question rides inside the same envelope. Kinetic simulations report electric potential-barrier structures in magnetic nozzles; whether analogous structures in an energy-recovery expander would reflect the very electrons one is trying to collect is not yet settled, and it is carried as part of the open-risk band rather than assumed away. This is the enabling result for both the paper's core and its IP position: a converter topology that recovers the *larger* axial channel without the wall of §3. THEORY / OPEN-RISK

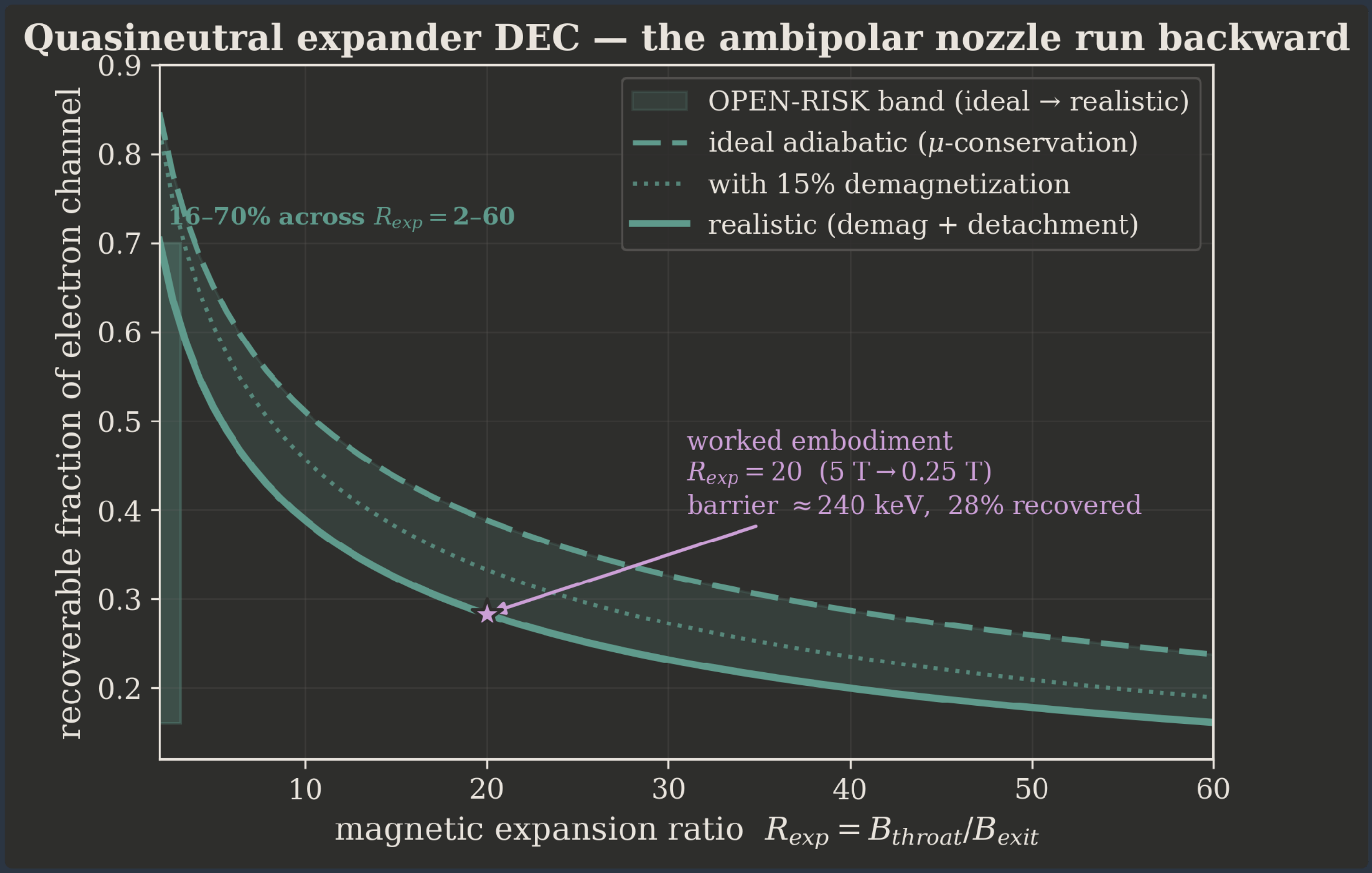

FIGURE 6. Recoverable electron-channel fraction versus magnetic expansion ratio. The shaded band spans the ideal adiabatic limit to the realistic case after demagnetization and detachment losses; the worked embodiment (R_{exp} = 20) recovers ≈28%. Basis: derived (adiabatic μ-conservation + ambipolar barrier); loss terms open-risk. THEORY / OPEN-RISK

§ 6

The path to demonstration — a pre-registered bench program

Because the recoverable fraction is the paper's one genuinely open-risk number, the honest move is to specify the experiment that closes it *before* building it — and to fix the falsification thresholds in advance, so the result cannot be read after the fact to flatter the model. That is the pre-registered X11–X12 bench program.

The key enabling fact is that the mechanism is governed by dimensionless invariants, not by absolute scale. An energy-recovery expander tests through three of them — $e\Delta\varphi/T_e = \ln R_{exp}$, the electron magnetization ρ_e/L, and the collisionality λ_{mfp}/L. A bench plasma matched to the reactor's electron magnetization and (collisionless) detachment regime measures the *same* dimensionless recovered fraction as the reactor, even though it runs four orders of magnitude colder.

BENCH ELECTRON TEMPERATURE	$T_e \approx$ **10 eV** — matched in the dimensionless invariants to the 80 keV reactor point
THROAT FIELD	$B_{throat} \leq$ **0.5 T** — buildable, ample diagnostic signal
EXPANSION RANGE	R_{exp} = **10–100**
FALSIFICATION — BARRIER	the ambipolar barrier must track $\ln R_{exp}$ to **±20%**
FALSIFICATION — RECOVERY	measured $f_{rec}(R_{exp})$ must fall within or above the model band, with quasineutrality preserved and no space-charge stall

A design-support scan confirms this operating box is reachable at buildable fields with ample diagnostic signal. The decision bands are drawn before the run (Figure 7). The logic is deliberately symmetric: a result that confirms the band converts §5 from a derived estimate to a measured quantity; a result that falls below the realistic curve *bounds* the recoverable fraction and still closes a named open problem in advanced-fuel energy conversion. **Either outcome is publishable, and either outcome advances the field** — a bounded-negative result is not a failure, it is a measurement. The absolute 80 keV reactor operating point remains a labeled extrapolation throughout; what the bench measures is the dimensionless mechanism, cleanly. OPEN-RISK → TO BE MEASURED

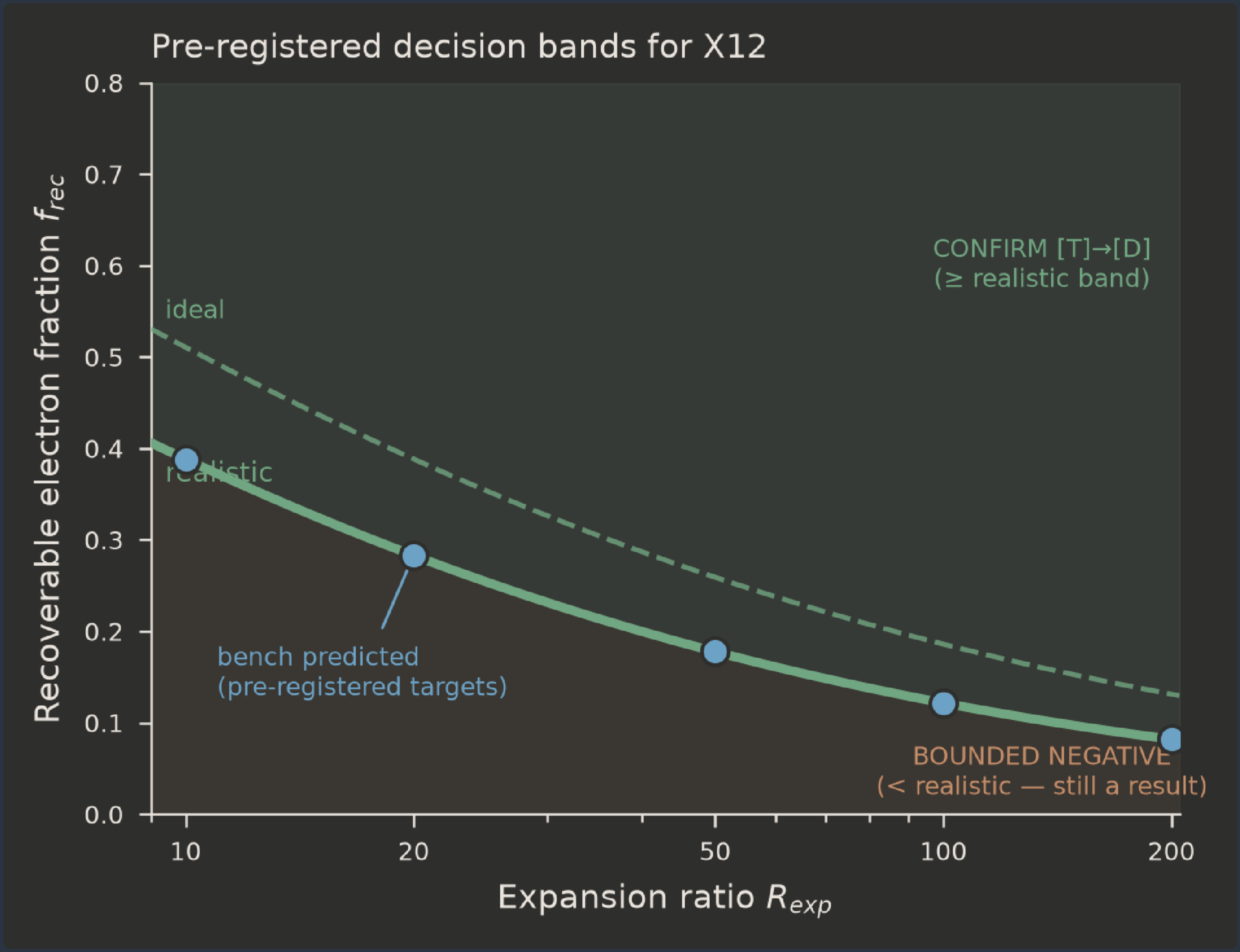

FIGURE 7. Pre-registered decision bands for the expander demonstration. The bench targets (blue) lie on the realistic model curve; a measured recoverable fraction in the green region confirms the mechanism, while a result below the realistic curve bounds it and still closes the open problem. Thresholds are fixed before the run. Basis: the design-support model and pre-registration in the deposit. OPEN-RISK → TO BE MEASURED

§ 7

Fuel spectrum and converter topology — why D–³He, not ³He–³He

The converter topology is fuel-dependent, and this is where the definitional result of the foundations — that a charged fusion product is not thereby a *directable* one — earns its keep. Deuterium–helium-3 delivers two discrete lines: a proton at **14.66 MeV** and an alpha at **3.67 MeV**, thermally broadened at 80 keV. A monoenergetic grid stack or a travelling-wave converter can decelerate two lines efficiently, because it can be tuned to sit where the energy actually is.

Helium-3–helium-3, the fully aneutronic alternative often held up as the ideal advanced fuel, does not cooperate. It is a **three-body reaction** — ^{4}He + 2p, Q = **12.86 MeV**, from AME2020 masses — whose two protons share the energy continuously, forming a broad continuum with a kinematic endpoint at **(5/6)Q ≈ 10.7 MeV**. A narrow-band grid stack cannot match a continuum; there is no single energy to tune to, so most of the spectrum lands off the acceptance window and is lost to heat. This is the same structural point as the proton–boron case in the foundations, made quantitative for a converter.

Modelling a retarding grid stage as a triangular fractional-acceptance window makes the penalty explicit (Figure 8):

10.5×	2.4×	12.86 MeV
D–³HE ADVANTAGE, NARROW BAND	D–³HE ADVANTAGE, WIDE BAND	³HE–³HE Q (AME2020)
two lines vs. three-body continuum	advantage persists even relaxed	endpoint (5/6)Q ≈ 10.7 MeV

At narrow bandwidth the D–^{3}He two-line spectrum recovers **≈10.5×** more than the ^{3}He–^{3}He continuum; even at wide bandwidth, where the grid stack is most forgiving, D–^{3}He still recovers **≈2.4×** more. This supports the D–^{3}He fuel choice and the grid-stack row of the ledger. The exact three-body spectral shape is modelled statistically and carried as open-risk — but the *conclusion* (two lines beat a continuum) is robust to the shape; only the precise ratio is uncertain. DERIVED (D–³HE) OPEN-RISK (CONTINUUM SHAPE)

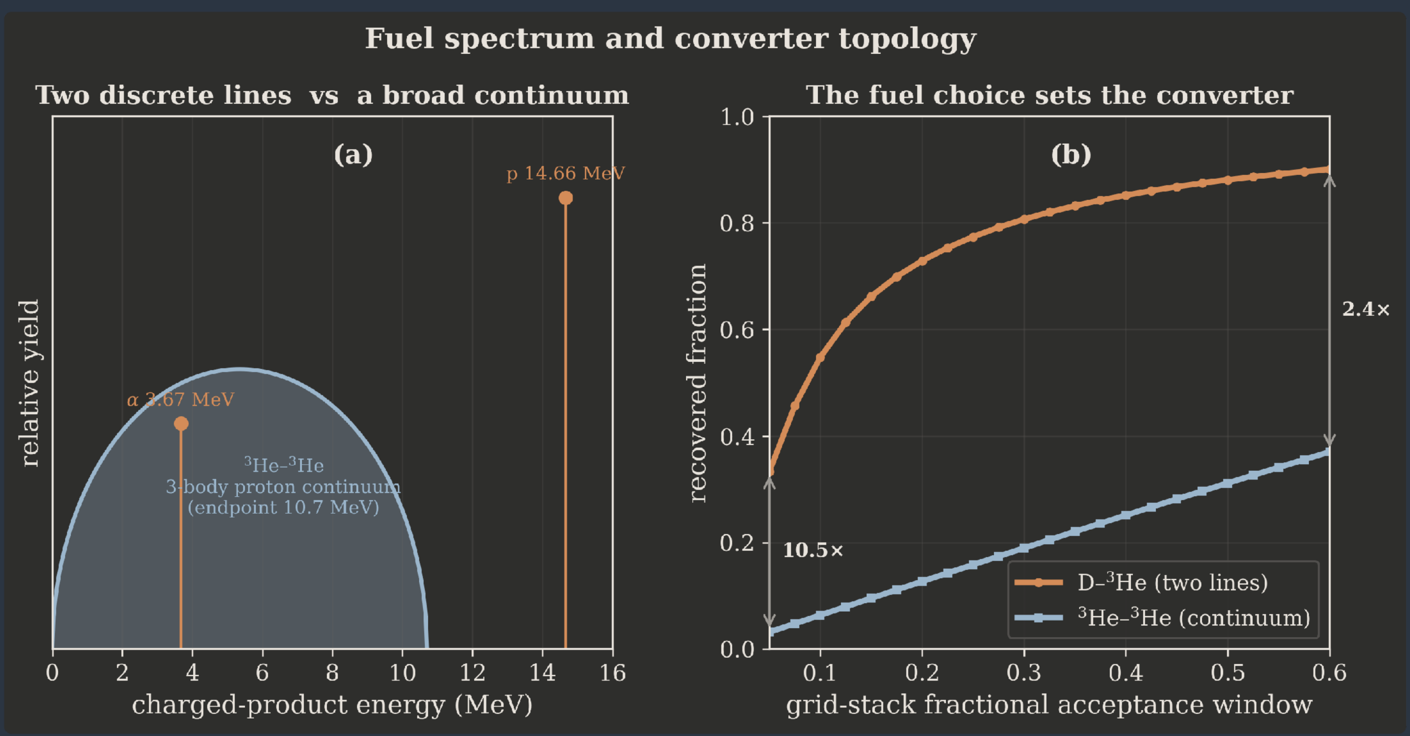

FIGURE 8. (a) The D–³He two-line spectrum versus the ³He–³He three-body proton continuum. (b) Grid-stack recovered fraction versus fractional acceptance window: D–³He dominates by 10.5× (narrow) to 2.4× (wide). Basis: derived (D–³He); continuum shape open-risk (³He–³He). DERIVED OPEN-RISK

§ 8

The honest ledger and the closure card

The per-stage efficiency ledger is banded and basis-tagged, so a reader can see exactly which stage rests on measured hardware and which on a derived open-risk number. Three stages carry the conversion:

TABLE 1 · MASTER PER-STAGE DEC LEDGER — NOMINAL EFFICIENCY WITH SOURCED/DERIVED BAND AND BASIS

STAGE	CHANNEL	H NOM.	BAND	BASIS
Ion DEC (venetian-blind / TWDEC)	ion	**0.48**	0.45–0.65	sourced — measured single-stage MEASURED
Electron → thermal bottoming (sCO_2)	electron	**0.45**	0.40–0.50	sourced — Brayton practice MEASURED
Electron → quasineutral expander (novel)	electron	**0.283**	0.16–0.40	derived, open-risk OPEN-RISK

The ion-DEC stage carries a sourced 0.45–0.65 band with a nominal of **0.48** — and that choice matters. The nominal is the *measured single-stage tube efficiency*, not the aspirational two-stage total; the band's high end traces to a report frequently available in abstract only, so the ledger uses the conservative measured figure and lets the optimistic end sit visibly in the band. The electron thermal-bottoming stage carries a sourced 0.40–0.50 (nominal **0.45**), standard supercritical-CO_2 Brayton practice. The expander stage carries a derived 0.16–0.40 (nominal **0.283**), flagged open-risk — the number from §5.

THE CASCADE — WHY 0.283 < 0.45 IS NOT A LOSING TRADE

The two electron-channel rows are *not* alternatives to be compared head-to-head. Reading 0.283 < 0.45 as "the expander loses to thermal bottoming" is the trap. They are a **cascade**: the expander tops the directed energy at collector efficiency η_{col} = 0.85, and the fraction it does *not* capture then bottoms thermally at η_{th} = 0.45. Nothing is thrown away.

The effective electron-channel efficiency is therefore the cascade sum:

$$\eta_e^{eff} = f_{rec}\,\eta_{col} + (1 - f_{rec})\,\eta_{th} = 0.283 \times 0.85 + 0.717 \times 0.45 = \mathbf{0.563}$$

0.563	0.85	0.45
CASCADE H_E^{EFF}	COLLECTOR H_{COL}	BOTTOMING H_{TH}
genuine gain over 0.45 thermal-only	expander tops the directed energy	remainder bottoms thermally

The cascade gives **0.563** — a genuine gain over the 0.45 thermal-only baseline, and the reason the expander is worth building even though its own stage efficiency looks low in isolation. Applying the cascade to the canonical axial split of §2 produces the ledger and closure card (Figures 9–10):

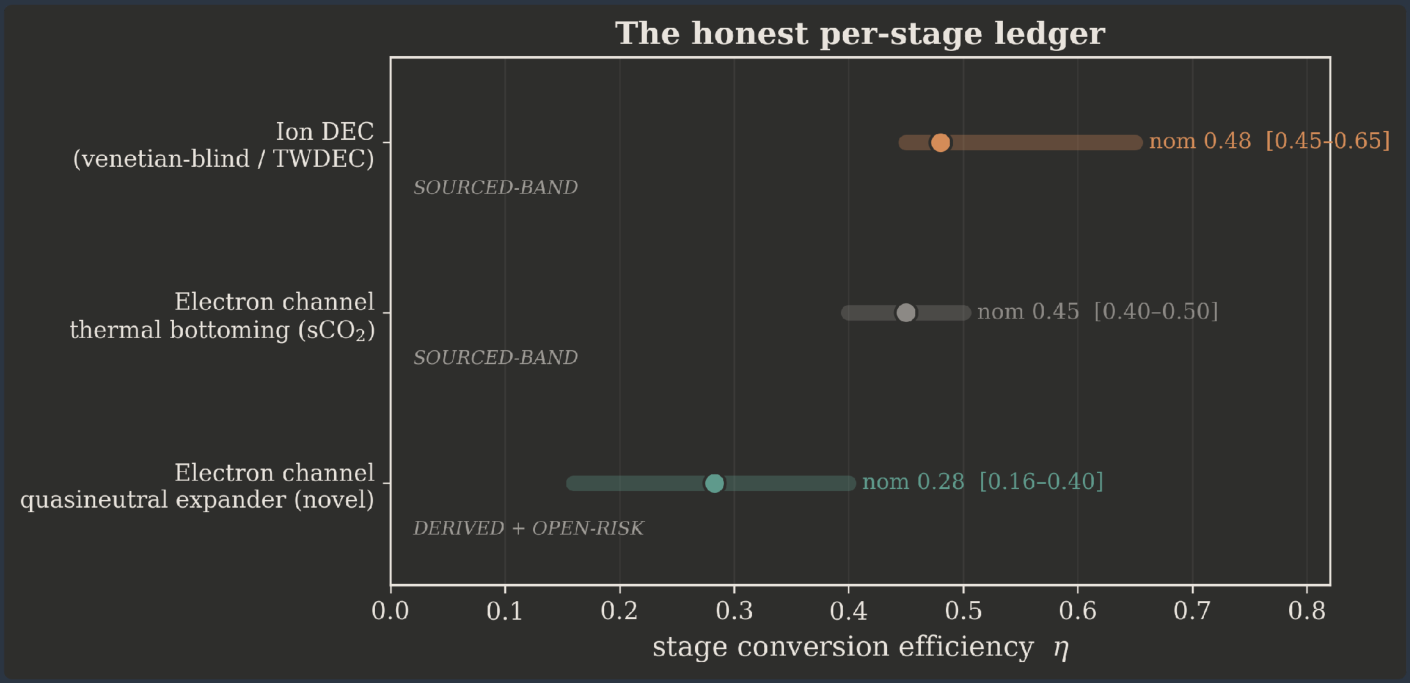

FIGURE 9. The per-stage ledger with sourced/derived bands — the ion DEC, electron thermal-bottoming, and novel expander stages, each shown with its band and basis tag. Basis: canon axial split (simulator) plus sourced/derived stage efficiencies. DERIVED

THE CLOSURE CARD — STATED WITHOUT INFLATION

The expander lifts axial electric recovery from **717.5 MW to 814.8 MW** — a **≈13%** gain, **≈97** $\mathbf{MW_e}$ on the electron channel. But the plant energy multiplication moves only from $\mathbf{Q_E = 1.0023}$ **to 1.0026**, because Q_E is set by the plug and thermal-barrier recirculating power, not by the DEC stage. DEC is a bounded upside lever, not the burner's closure mechanism.

We state this deliberately, against the temptation to present the expander as the difference between $Q_E \approx 1$ and a large multiple. It is not that. Its value is that it recovers the dominant axial channel through a route with no known wall, and that a bounded experimental result on it — positive or negative — resolves a standing open problem. The 97 MW_e is real electricity; the Q_E needle barely moving is the honest ceiling on what that electricity is worth to the plant balance. Both facts are on the card. DERIVED OPEN-RISK

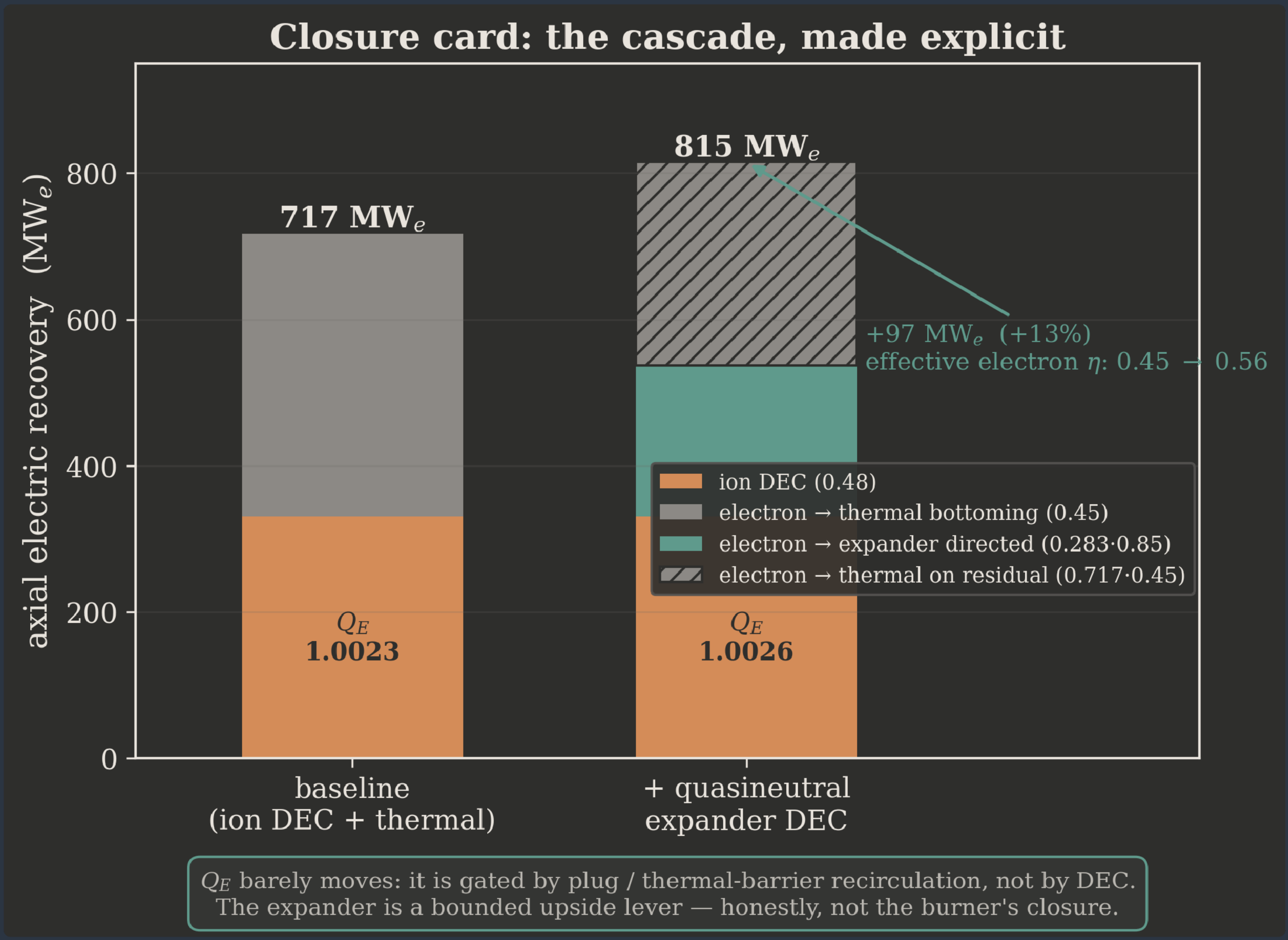

FIGURE 10. The closure card with the cascade made explicit. The expander adds ≈97 MW_e on the electron channel (717.5 → 814.8 MW), but Q_E moves only from 1.0023 to 1.0026 — it is gated elsewhere in the burner, by the plug/thermal-barrier recirculating power. Basis: canon axial split (simulator) plus sourced/derived stage efficiencies. DERIVED OPEN-RISK

The 97 megawatts is real electricity; the Q_E needle barely moving is the honest ceiling on what it is worth.

§ 9

Limitations — four open-risks, carried rather than absorbed

The value of this paper is inseparable from the discipline of naming what it does not yet know. Four open-risks are carried explicitly, each with the statement of what closes it.

(I) EXPANDER RECOVERABLE FRACTION	Depends on demagnetization and detachment losses located by the propulsion literature but *not measured* for an energy-recovery expander; carried as the band ideal 0.39 → realistic 0.28. **Closed by** the pre-registered X11–X12 bench program of §6.
(II) SIGNAL CURRENT J_{SIGNAL}	A simulator operating point, not a measured collector value. The back-emission-wall conclusion is *robust* to it — the real-emitter band floods by 10^1–10^4× — but the exact contour position is not pinned.
(III) ^{3}HE–^{3}HE SPECTRAL SHAPE	Modelled statistically. The two-line-beats-continuum *conclusion* is robust; the precise 10.5×/2.4× ratio is open-risk.
(IV) ION-DEC BAND HIGH END	The 0.65 top traces to a report frequently available in abstract only; the ledger uses the measured single-stage **0.48**, the conservative choice.

None of these four undermines a headline conclusion. Each attaches to a *number* inside a conclusion whose *direction* is independently robust: the split is electron-dominant regardless of κ (i, via the split's robustness); the wall floods every real emitter regardless of the exact J_{signal} (ii); D–^{3}He beats the continuum regardless of its exact shape (iii); and the ledger's ion stage is anchored on the measured, not the aspirational, figure (iv). The open-risks are quantitative, not structural. OPEN-RISK

§ 10

Conclusion — the problem is not the one the birth spectrum suggests

The DEC problem for a deuterium–helium-3 mirror burner is not the one the birth spectrum advertises. At reactor temperature the electron/thermal channel is the *larger* axial stream, not the small remainder; no established converter recovers a directed electron stream, because the hot-emitter route is walled off by its own thermionics; and the quasineutral two-species expander — the ambipolar nozzle run backward for energy recovery — is a route to recovering that channel that has not been proposed before. Every enabling piece is individually established — adiabatic conversion, the ambipolar nozzle, quasineutral two-species flow — and none has ever been assembled in reverse for this purpose.

We have bounded what it can deliver without inflation. The upside is real but modest on plant Q_E (1.0023 → 1.0026), because Q_E is gated by physics elsewhere in the burner; the electron-channel electricity it recovers (≈97 MW_e, a ≈13% lift) is genuine; and the one open-risk number that carries the concept — the recoverable fraction — is attached to a pre-registered bench experiment that closes it either way. A confirming result promotes the concept from derived to measured; a bounding result still resolves a named open problem in advanced-fuel energy conversion. The correction and the concept stand on their own, and the payoff is stated at its true size, not a larger one.

PROVENANCE

This architecture descends from the D–^{3}He direct-energy-conversion program developed by G L Kulcinski and colleagues at the University of Wisconsin–Madison; the present work implements and extends that lineage and cites it as provenance, not as arm′s-length prior art. Every number and figure is regenerable from first-principles scripts reading a declared operating-point table; the code, data, prior-art ledger, and the pre-registered X11–X12 experiment design (physics only) are archived at Zenodo (doi:10.5281/zenodo.21842864), and the companion breeder and burner deposits′ engines run live in the browser. No external laboratory, program, award, or partnership is represented as validating or funding this work, and **Kronos has built no converter.** Provisional patent applications relating to aspects of this work have been filed.

Portfolio, People & Record

The intellectual-property estate, the people who built it, the limitations that gate it, and the sources it rests on.

1	4	40	27
GRANTED PATENT	2026 PROVISIONALS	TEAM MEMBERS	2022 PROVISIONALS

INTELLECTUAL PROPERTY

The patent portfolio

The estate spans a granted high-field magnet patent, pending utility and 2026 provisional filings that map to the two products, a digital-twin control provisional, a registered trademark application, and the original 2022 provisional family. Every patentable disclosure in the five-paper arXiv drop was protected **before** publication: the breeder and burner provisionals were filed 1–2 August, and a publication-gap omnibus filing the evening before the drop swept up the DEC, plasma-control, and REBCO-winding matter of the three otherwise-unprotected papers. Patent numbers and application serials are matters of public record; claim scope is summarised, not reproduced.

GRANTED & PENDING UTILITY

US 12,009,112	High-field tilted graded-REBCO magnet architecture (KRONO-002A) · *app. 17/878,550*	GRANTED
US 17/878,507	Core device / method (KRONO-001A) · *utility*	PENDING

2026 PROVISIONAL FILINGS — MAPPED TO THE PRODUCTS

64/124,209	Hyperion — spherical-tokamak tritium / helium-3 foundry · *breeder · filed Aug 2026*	FILED
64/124,220	Aegis / MetroVolt — synchrotron-cutoff, fuel-selection & plug-winding · *generator · filed Aug 2026*	FILED
64/115,167	KRONOS-CTRL digital-twin plant control · *provisional · filed Jul 2026*	FILED
64/005,440	Integrated spherical-tokamak fusion architecture · *early integrated-architecture filing · filed Mar 2026*	FILED
64/105,530	Negative-triangularity spherical-tokamak architecture · *foundational ST filing · filed Jul 2026*	FILED
64/128,097	Publication-gap omnibus — quasineutral two-species expander DEC · provenance-gated / latency-split plasma control · as-built high-field winding & conductor architecture · *filed 7 Aug 2026, the evening before the arXiv drop*	FILED

TRADEMARK & ORIGIN

FTK-98801894	Kronos Fusion Energy — trademark application	FILED
KR-2022-*	Original provisional family (KR-2022-00001 … 00027) · *27 filings, 2022*	PRIORITY

The narrow, defensible magnet novelty — the specific conductor and the digital-twin winding optimisation, not high-field REBCO as a category — is the commercial core that can earn ahead of any Q > 1 milestone, with markets in fusion magnet supply, MRI/NMR, accelerators, and proton therapy. The claim is scoped honestly: the high field is a *system field* result, not a stand-alone-coil record; the small-bore plug coil is structurally infeasible as a bare winding but resolved by a stress-managed structural shield (feasible-pending-FEA); and the winding-tape experiment returned a *null result*. The value is the method, not a field record.

THE TEAM

Founding partners, board, advisors & auditors

Kronos is built by a bench of advanced-fuel-fusion, high-field-magnet, direct-conversion, and materials specialists, with a board and operations team drawn from defense, national laboratories, and industry. Dates are shown as ranges; where a tenure has ended or is term-ending, the range says so.

FOUNDING PARTNERS — SCIENCE

Dr. Gerald Kulcinski
Co-Founder · Helium-3 & Advanced-Fuel Fusion
UW–Madison · 2023–Present

Dr. Carl Weggel
Chief Scientist / S.M.A.R.T. Design
MIT Alcator Program · 2022–Present

Dr. Robert J. Weggel
Magnetic Field Design
MIT Magnet Lab · 2022–Present

BOARD

Priyanca Ford
Founder & CEO · Executive Board
2022–Present

Bandel Carano
Finance / Strategy
Oak Investment Partners / Stanford · 2025–2026

Patrick Schweiger
Fusion Device Engineering
Oklo / CFS / TerraPower · 2025–Present

SCIENTIFIC ADVISORS

Dr. Steven O. Dean
Fusion Policy & History
DOE / Fusion Power Associates · 2025–Present

Dr. Patrick H. Diamond
Plasma Turbulence & Transport
UC San Diego · 2025–Present

Dr. Jack J. Dongarra
HPC & Numerical Algorithms
Turing Award · 2025–Present

Dr. Nasr M. Ghoniem
Chief Material Scientist
UCLA · 2025–Present

Dr. Siegfried Glenzer
Plasma Physics & Laser Fusion
Stanford / SLAC · 2022–Present

Dr. David A. Hammer
Pulsed-Power Fusion
Cornell · 2025–Present

Dr. Donald A. Spong
Plasma Theory & Confinement
ORNL · 2025–Present

Dr. Curtis Smith
Risk Assessment & Nuclear PRA
MIT / Idaho National Lab · 2025–Present

RADM (Ret.) David Goggins
Naval Engineering & Power-Plant Design
U.S. Navy · 2023–2026

Dr. Konstantin Batygin
Mathematician
Caltech · 2022–2025

Dr. Ruben Fair
Magnet Design / ITER Liaison
PPPL / Jefferson Lab · 2022–2025

Dr. Paul S. Weiss
Materials & Nanotechnology
UCLA · 2022–2025

SCIENTIFIC AUDITORS

Dr. Wilfred A. Cooper
Plasma Equilibrium Theory
EPFL / Swiss Plasma Center · 2025–Present

Dr. Ahmed Hassanein
Plasma–Material Interactions
Purdue / Argonne · 2025–Present

Dr. Patrick E. Hopkins
Extreme Thermal Materials
U. of Virginia · 2025–Present

Dr. Peter Hosemann
Materials Joining & Structural Integrity
UC Berkeley · 2025–Present

Dr. Travis W. Knight
Advanced Nuclear Fuels & Systems
U. of South Carolina · 2025–Present

Dr. Philippe Lebrun
Cryogenics & Magnet Cooling
CERN · 2025–Present

Dr. Nitendra Singh
Nuclear Safety & Fuel Cycle
ITER · 2025–Present

Dr. Guido Van Oost
Magnetic Confinement & Fusion Systems
Ghent University · 2025–Present

Dr. Gary S. Was
Radiation Materials & Structural Integrity
U. of Michigan · 2025–Present

Dr. Ray Sedwick
Direct Energy Conversion
U. of Maryland · 2025

OPERATIONS

Michael Laughlin
Chief Operating Officer
2022–Present

Martin Owens
Chief Strategy Officer
LANL / GE Hitachi · 2022–Present

MG (Ret.) Paul Pardew
Chief Contracting Officer
Army Contracting Command · 2022–Present

David Beck
Fusion Commercialization
U.S. Space Force · 2024–Present

Sushma Bhatia
Environmental & Legislative
Google · 2022–Present

Michael De Frenza
Technology Licensing
2023–Present

MG (Ret.) Robin L. Fontes
Cybersecurity & Defense
Army Cyber Command · 2022–Present

Vijay Gehani
Supply Chain & Components
INOX India · 2024–Present

Jon Michel Greenwood
IT & AI Infrastructure
Live Nation · 2023–Present

Brian C. O'Neill
National Security
CIA / ODNI · 2022–Present

Gen. (Ret.) Gustave F. Perna
DoD Liaison
Operation Warp Speed · 2022–2023

Andrea Romero
Marketing Lead
2022–Present

Legal counsel is retained; those roles are held on the internal roster and are not listed here.

LIST OF FIGURES

List of Figures

LIST OF TABLES

List of Tables

REFERENCES

Sources

[1] H.-S. Bosch and G. M. Hale, "Improved formulas for fusion cross-sections and thermal reactivities," *Nuclear Fusion* **32**, 611 (1992).

[2] A. S. Richardson, *NRL Plasma Formulary*, Naval Research Laboratory (2019).

[3] I. E. Ochs, E. J. Kolmes, and N. J. Fisch, "Bremsstrahlung and the electron–electron contribution in fusion plasmas," *Physics of Plasmas* (2024).

[4] T. H. Rider, "Fundamental limitations on plasma fusion systems not in thermodynamic equilibrium," *Physics of Plasmas* **4**, 1039 (1997).

[5] ITER Physics Expert Groups, "ITER Physics Basis," *Nuclear Fusion* **39**, 2137 (1999).

[6] N. A. Uckan and J. Sheffield, "Tokamak scaling and confinement," in *Tokamak Concept Improvement*, IAEA (1989).

[7] O. Sauter, C. Angioni, and Y. R. Lin-Liu, "Neoclassical conductivity and bootstrap current," *Physics of Plasmas* **6**, 2834 (1999).

[8] F. Troyon *et al.*, "MHD limits to plasma confinement," *Plasma Physics and Controlled Fusion* **26**, 209 (1984).

[9] J. P. Freidberg, *Plasma Physics and Fusion Energy*, Cambridge University Press (2007).

[10] R. F. Post, "The magnetic mirror approach to fusion," *Nuclear Fusion* **27**, 1579 (1987).

[11] D. E. Baldwin, "End-loss processes from mirror machines," *Reviews of Modern Physics* **49**, 317 (1977).

[12] T. K. Fowler, R. W. Moir, and T. C. Simonen, "A new simpler tandem mirror," *Nuclear Fusion* **57**, 056014 (2017).

[13] G. L. Kulcinski and J. F. Santarius, "Advanced fuels and the D–^{3}He cycle," University of Wisconsin Fusion Technology Institute.

[14] W. L. Barr and R. W. Moir, "Test results on direct energy converters for mirror reactors," *Nuclear Technology/Fusion* **3**, 98 (1983).

[15] D. B. Go *et al.*, "Thermionic energy conversion in the twenty-first century," *Frontiers in Mechanical Engineering* **3**, 13 (2017).

[16] M. Wang *et al.*, "The AME 2020 atomic mass evaluation," *Chinese Physics C* **45**, 030003 (2021).

[17] J. E. Menard *et al.*, "Fusion nuclear science facilities and pilot plants based on the spherical tokamak," *Nuclear Fusion* **56**, 106023 (2016).

[18] A. J. Creely *et al.*, "Overview of the SPARC tokamak," *Journal of Plasma Physics* **86**, 865860502 (2020).

[19] T. P. Wright, "Factors affecting the cost of airplanes," *Journal of the Aeronautical Sciences* **3**, 122 (1936).

[20] U.S. Department of Energy / NNSA, *Stockpile Stewardship and Management Plan*, FY2024.

[21] J. F. Santarius, G. L. Kulcinski, and L. A. El-Guebaly, "A strategy for D–^{3}He fusion energy development," *Journal of Fusion Energy* **17**, 33 (1998).

[22] M. A. Abdou *et al.*, APEX advanced blanket concepts, *Fusion Engineering and Design* (1999–2003).

[23] Federal Register, notice on supply of tritium to non-federal entities (1999).

[24] Kronos Fusion Energy, "Simulation register and reproducibility deposit," Zenodo (2026).

[25] A. O. Thome *et al.*, "ELM-free negative-triangularity edge on DIII-D," *Plasma Physics and Controlled Fusion* (2024), doi:10.1088/1361-6587/ad6f40.

[26] T. Eich *et al.*, "Scaling of the tokamak near scrape-off layer power width," *Nuclear Fusion* **53**, 093031 (2013).

[27] J. Lim *et al.*, "Scrape-off-layer width in negative-triangularity plasmas," *Nuclear Fusion / Plasma Physics and Controlled Fusion* (2023).

[28] A. O. Nelson *et al.*, "Prohibition of second-stability access at negative triangularity," *Plasma Physics and Controlled Fusion* **64**, 124002 (2022).

COLOPHON

How this document was made

The Kronos Fleet — Combined Editorial, 2026 is set in **Fraunces** (display), **Gelasio** (text), and **IBM Plex Mono** (data & equations), carried forward from the Kronos editorial design system.

The figures are rendered at 300 dpi from the deposited generator scripts; the document is composed as a single self-contained file with embedded fonts and imagery, paginated to US Letter, and rendered to PDF through a headless Chromium engine in matched light and dark editions.

Every headline quantity carries an evidence class; withdrawn and restated values are marked as such. Nothing herein is frozen beyond the founder-approved Tier-A set.

Explore it live — turn the interactive 3-D model, run the deposited solvers in the physics validator, and watch the companion film series.

◆

LEGAL NOTICE

Notice, status, and distribution

Conceptual design & simulation study. This document reports a conceptual design and simulation study. It is not a construction commitment, a safety-analysis report, a regulatory filing, or an offer of securities. Forward-looking statements — schedules, costs, market sizes, and performance — are estimates subject to the limitations set out in the Simulations part and may change.

Numbers and their classes. Quantities are reported with evidence classes and case labels; modelled, assumed, and requirement-class values are identified as such and are not to be quoted without their labels.

Public edition. This edition carries the physics and design only; all financial, funding, and defense-commercial content has been removed for public distribution. The scientific text corresponds to the arXiv and journal submissions.

THE 2026 KRONOS SET

One programme, in five papers

This editorial is one of five that together describe the Kronos fusion programme — a breeder that funds a generator, and the magnet, conversion, and control science that enable both. Each is published open-access with a reproducible companion deposit.

PAPER I	**Hyperion — The Tritium Foundry** · 10.5281/zenodo.21746157
PAPER II	**Aegis & MetroVolt — The Generator** · 10.5281/zenodo.21746479
PAPER III	**High-Field REBCO Magnets & Tape** · 10.5281/zenodo.21842514
PAPER IV	**Direct Energy Conversion** *(this paper)* · 10.5281/zenodo.21842864
PAPER V	**AI, ML & Quantum Control** · 10.5281/zenodo.21842371

Explore the whole programme live: the interactive 3-D model, the in-browser physics validator, and the companion film series.

KRONOS FUSION ENERGY

Direct Energy Conversion

Explore the science — live, in your browser.

kronosfusionenergy.com/3D-Model

kronosfusionenergy.com/physics-Validation-Simulation

Companion film series · YouTube

Zenodo · DOI 10.5281/zenodo.21842864

